Desalination and Water Treatment
www.deswater.com

doi: 10.5004/dwt.2019.24084

154 (2019) 30–38
June

Chromium removal by forward osmosis: a flux modeling and experimental validation

Dhouha Ben Maouia[a,*], Ali Boubakri[a], Raja Bouchrit[a], Amor Hafiane[a], Salah Bouguecha[b]

[a]*Laboratory of Water, Membrane and Biotechnology, CERTE, P.B. 273, 8020 Soliman, Tunisia, Tel. +216 50971194; email: dhouha.benmaouia@gmail.com (D.B. Maouia)*
[b]*Department of Mechanical Engineering, Faculty of Engineering, King Abdulaziz University, P.B. 80204, Jeddah 21589, Saudi Arabia*

Received 2 April 2018; Accepted 2 March 2019

ABSTRACT

Chromium is one of the most widely used heavy metals in industry as it has enough advantages for tanneries, textiles, wood processing and agro-food industries. Chromium VI is highly toxic and highly soluble in water, which is the origin of its great mobility in the ecosystems. In this study, the forward osmosis (FO) process was investigated to remove chromium from aqueous solution using cellulose triacetate membrane and ammonium bicarbonate (NH_4HCO_3) as draw solution. The effect of various operating parameters such as feed temperature, feed concentration, draw temperature and draw concentration on FO performance was evaluated. The experimental runs showed that the permeate flux was enhanced with draw temperature, and maximum permeate flux of 2.38×10^{-6} m s^{-1} was obtained at 55°C. The permeate flux was found to decrease with feed concentration. Moreover, the flux reached 2.9×10^{-6} m s^{-1} at maximum draw concentration of 3 mol L^{-1}. These operating parameters had insignificant effect on chromium rejection and reached, in all cases, more than 99%. The validation of the model, using McCutcheon and Elimelech model, shows a good agreement with the determined experiment alones.

Keywords: Forward osmosis; CTA membrane; Chromium retention; Water flux; Modeling

1. Introduction

Toxic metal pollution is one of the most important environmental problems worldwide. Examples are heavy metals such as chromium, manganese, iron, zinc and cadmium, which are widely used in various industries due to their highest processibility. The residual waters are contaminated, and therefore dangerous to human health and potential pollutants for the environment [1].

Chromium is the most toxic and the most prevalent mutagen of the used metal ion in biological systems. Its use has gradually increased by industrial activities such as catalysts, pigments, alloys, corrosion inhibition, leather tanning, metallurgy, electroplating, petroleum refining, textile manufacturing and pulp production. Chromium compounds mainly exist as trivalent Cr(III) and hexavalent Cr(VI) in the environment. The exposure of both forms to the environment is common and emanates from natural and industrial sources. It is well known that Cr(VI) is much more mobile, 300 times more toxic and more carcinogenic than Cr(III) [2]. The soil is most affected with 900 ton of chromium rejected per year, the surface waters with about 140 ton year^{-1} and the atmosphere with 30 ton year^{-1} [1]. Consequently, the removal of chromium from water is necessary in order to safeguard public health and environment.

Several methods are available to separate the chromium from wastewaters such as activated carbon [3], chemical precipitation [4], ion exchange [5], liquid–liquid extraction [6], adsorption [7] and biosorption [8]. However, these techniques are unable to reach a high retention ratio (99.95%) required by the standard norms established by the World Health Organization. The disadvantages of these methods

* Corresponding author.

are to produce large quantities of toxic chemical sludge, whose disposal constitutes a major problem [9].

In addition, membrane processes such as reverse osmosis and nanofiltration have also been applied for this purpose. However, the fast permeate declines due to the existence of suspended solids. Besides, the oxidized compounds in the wastewater cause irreversible fouling on the surface of the reverse osmosis membrane, which increases the operational costs due to the membrane replacement. Therefore, the nanofiltration is unable to ensure a high retention rate of chromium [10]. Hence, both processes are operated at high pressures and have relatively low water recovery rates, and therefore require comparatively high costs and suffer the risk of severe membrane fouling.

Recently, forward osmosis (FO) is a suitable alternative process to the above-mentioned methods. It is an emerging technology that has garnered an increasing amount of attention in recent years. FO involves the transport of water from an aqueous solution of lower osmotic pressure on the feed solution (FS) (diluted solution) to a higher osmotic pressure draw solution (DS) (more concentrated solution), inducing the driving force for the separation across a semi-permeable membrane where the contaminants in the FS are rejected.

FO is preferred due to its expected advantages, such as the removal effectiveness, low pressure operation, low membrane fouling, lower costs and low power consumption, as appropriate draw solute and regeneration methods which constitute the most attractive aspect for the FO, particularly under the pressure energy crisis [11].

Therefore, application of FO membranes offers many advantages in the field of heavy metals removal. Recent advancement makes it realistic to support that FO might be one of the most reliable technologies to lower the energy consumption as compared with pressure-driven membrane processes. Despite all these advantages, FO has some drawbacks, namely the significant lower water flux obtained compared with the other processes, inefficiency of FO membranes and the absence of profitable draw solutes that can be easily recovered. Some previous works have showed the feasibility of FO based on its special characteristics, that is, low energy consumption, high rejection for a wide range of contaminants.

However, the research on the removal of chromium from water, using FO process, is still needed. In fact, to the best our knowledge, only research on the removal of heavy metals other than chromium has been undertaken. Cui et al. [12] have investigated the removal of six heavy metal solutions $Na_2Cr_2O_7$, Na_2HAsO_4, $Pb(NO_3)_2$, $CdCl_2$, $CuSO_4$, $Hg(NO_3)_2$ by FO using a thin-film composite (TFC) FO membrane. Their study has shown almost complete heavy metals rejections (higher than 99.7%) with a maximum permeate flux around 4.58×10^{-6} m s^{-1} by operating the FO process at 60°C. Vital et al. [13] applied FO process to remove Co(II), Cu(II) and Zn(II) from acid mine drainage using a TFC FO membrane. Their study showed that the FO process successfully removed the previously mentioned heavy metals with rejection rate of 99.0%, 98.0% and 99.9%, respectively, by using 1.0 mol L^{-1} NaCl as the DS. Zhao et al. [14] have studied the performance of FO in the removing of nickel (Ni^{2+}) using two different FO membranes (cellulose triacetate [CTA] and polyamide-based TFC membrane). They have reached a nickel removal of more than 93%. Liu et al. [15] have investigated the performance of Co(II) removal from aqueous solution by FO using a CTA membrane. Their study has successfully rejected the cobalt metal with the rejection rate more than 95% with water flux of 4.3×10^{-6} m s^{-1} when 1.0 mol L^{-1} of NaCl was used as a DS.

Some research works have focused on modeling water flux for FO process. Among these models, we can cite that developed by Lee et al. [16], Loeb et al. [17], which introduced a simplified equation to describe the water flux during FO without considering membrane orientation [18]. Another model is that developed by McCutcheon and Elimelech [19] for water flux using a dense symmetric membrane.

Therefore, the objectives of this study are to study the effects of experimental factors including draw concentration, feed concentration, draw temperature and feed temperature on the performance of FO process, using CTA membrane and ammonium bicarbonate as DSs. This study may also develop a model for the water flux and compare the experimental results with the predicted permeate fluxes.

2. Modeling of water flux

Osmosis is the natural diffusion of water through a semi-permeable membrane driven by the osmotic pressure difference. The osmotic pressure equation developed by Van't Hoff is widely used [20]:

$$\pi = nCRT \tag{1}$$

where n is the Van't Hoff factor (accounts for the number of individual particles of a compound dissolved in the solution), C is the molar concentration of the solution (mol L^{-1}), R is the gas constant (R = 0.0821 L atm mol^{-1} K^{-1}) and T is the absolute temperature (in K) of the solution.

In FO process, water from the feed moves toward the highly concentrated DS (leaving behind the solutes) due to the osmotic pressure gradient, when a semi-permeable membrane separates the two solutions. The water flux (J_w) in the FO process is given by:

$$J_w = A\sigma\left[\pi_D - \pi_F\right] \tag{2}$$

where A is the membrane pure water permeability coefficient, s is the reflection coefficient, and π_D and π_F are the osmotic pressures of the DS and FS, respectively.

Eq. (2) is valid only for dilute solutions and neglected concentration polarization (CP) phenomena which may be valid only if the permeate flux is very low. However, CP phenomena play a vital role in FO process.

The presence of two independent solutions on each side of the membrane results in two different types of CP: internal CP inside membrane and external CP within membrane–solution interface. In our study, because the active layer of the FO membrane was placed against the FS, dilutive internal CP would occur within the porous support, and therefore the water flux (J_w) of the FO process was simulated using a model developed by McCutcheon and Elimelech and calculated using the MATLAB software:

$$J_w = A\left[\pi_D e^{(-J_w K)} - \pi_F e^{(J_w/k)}\right] \tag{3}$$

where A is the permeability coefficient and its value varied with temperature presented in Table 1; π_D and π_F are the osmotic pressures of the DS and FS, respectively; K is the solute resistivity for diffusion within the porous support layer; and k is the mass transfer coefficient.

K is, therefore, a measure of effectiveness of the solute to diffuse into and out of the support layer which is defined as:

$$K = \frac{t\tau}{D_D}\varepsilon = \frac{S}{D_D} \tag{4}$$

where t, τ and ε are the thickness, tortuosity and porosity of the support layer, respectively. While t, τ and ε are membrane characteristics; S is a structural parameter of the membrane; D_D is a diffusion coefficient of draw solute and its value depends on the types of draw solutes and the temperature used. This diffusion coefficient can be calculated empirically using the Stokes–Einstein relationship [22]:

$$D_D = \frac{T_D k_b}{6\pi r\rho\vartheta} \tag{5}$$

where k_b is the Boltzmann constant, ϑ is the kinematic viscosity of the solution, T_D is the temperature of the DS, r is the ion radius, and ρ is the density of the solution as function of its molar concentration and temperature calculated by:

$$\rho = \rho_w + 0.261\times10^{2}C - 0.1577C\left(T-273\right) + 1.553\times10^{-3}C\left(T-273\right)^{2} - 2.556C^{1.5} + 5.67\times10^{-2}C^{1.5}\left(T-273\right) - 5.082\times10^{-4}C^{1.5}\left(T-273\right)^{2} \tag{6}$$

where ρ_w is the water density according to the empirical equation:

$$\rho_w = 999.65 + 2.0438\times10^{-1}\left(T-273\right) - 6.174\times10^{-2}\left(T-273\right)^{3/2} \tag{7}$$

where ϑ is defined by:

$$\vartheta = \frac{\mu}{\rho} \tag{8}$$

where μ is the dynamic viscosity calculated by:

$$\mu = 2.414\times10^{\left(\left(247.8/\left(T-140\right)\right)-5\right)} \tag{9}$$

Table 1
Water permeability coefficient at different temperatures [21]

T (K)	A (m Pa^{-1} s^{-1})
298	1.325×10^{-12}
302	1.38×10^{-12}
312	1.69×10^{-12}
321	1.9×10^{-12}
328	1.94×10^{-12}

And k is the mass transfer coefficient which is given by the following relationship:

$$k = \mathrm{Sh}\frac{D_F}{d_h} \tag{10}$$

where D_F is the diffusion coefficient of the feed solute defined as:

$$D_F = \frac{T_F k_b}{6\pi r\rho\vartheta} \tag{11}$$

And d_h is the hydraulic diameter of the flow channel defined as:

$$d_h = \frac{4S}{P_w} \tag{12}$$

where S is the area of the flow section and P_w is the hydrated perimeter.

Sh refers to the Sherwood number given by the following relationship based on the flow conditions in the channel:

$$\mathrm{Sh} = 1.85\times\left(\mathrm{Re}\times\mathrm{Sc}\frac{d_h}{L}\right) \tag{13}$$

where Re is the Reynolds number, Sc is the Schmidt number and L is the channel length of FO test cell. The Schmidt number and the Reynolds number can be determined by the following relationship:

$$\mathrm{Re} = \frac{\left(L\times v\times\rho\right)}{\mu} \tag{14}$$

where v is the average flow velocity.

Schmidt number defined by:

$$\mathrm{Sc} = \frac{\vartheta}{\rho D_F} \tag{15}$$

The osmotic pressures of the bulk DS (π_D) and FS (π_F) were calculated according to the Van't Hoff equation.

3. Materials and methods

3.1. Membrane and membrane characterization methods

Experiments were carried out using a membrane consisting of a very thin semi-permeable nonporous active skin layer of CTA embedded in a nylon mesh (a porous support layer) provided by Hydration Technologies Innovations (HTI OsMem™ CTA-NW Membrane). Table 2 shows its operating limits as specified by manufacturer.

The membrane characterization was performed using the following methods:

- FEI Quanta FEG 250 scanning electron microscope (SEM) characterizes the CTA membrane morphologies.
- The Attension Theta optical tension-meter determines the membrane hydrophobicity character via the measurement of the membrane contact angle (CA).

Table 2
Operating limits of CTA membrane

Membrane type	Cellulose triacetate (CTA) on heat-or RF-weldable nonwoven support
Maximum operating temperature	159.8°F (71°C)
Maximum trans-membrane pressure	10 psi (70 KPa), if supported
pH range	3 to 8
Maximum chlorine	2 ppm

- Zygo newview 7100 profilometer investigates the surface roughness of the membrane and gives an idea about the membrane shape surface in three-dimensional details.
- PerkinElmer spectrum 100 FTIR spectrophotometer determines the chemical composition of the membrane.

The CA measurement (Fig. 1a) made for virgin membrane surface was equal to 76°. This confirms that the used membrane is hydrophilic because it is known that a CA of 0° corresponds to an ideal hydrophilic membrane surface and the increase of this CA enhances their hydrophobicity [23]. This hydrophilic character is beneficial to the permeation of water and can enhance antifouling tendencies in application.

Fig. 1b shows the SEM image obtained for the membrane with magnification = 40 μm, where the microstructures of the membrane surface can be easily observed. Here, the active layer of CTA-NW seems to be dense and less porous.

Fig. 1c reveals that the characterized membrane has a maximum and average surface roughness = 10.117 and 1.560 mm, respectively. This roughness allows for a drop of fixed volume to spread by capillary action into the crevices on the surface. The spreading is facilitated by the hydrophilicity of the polymer and improves the capillary movement of water not only into these crevices but also into the pores within the membrane. Hence, this will give the appearance of a lower CA. At the same scale, the surface of asymmetric CTA-NW membranes was quite smooth which implies lower potential of fouling propensity of the membrane.

Fourier transform infrared spectroscopy (FTIR) analysis is shown in Fig. 1d. The peaks at 925.23 and 871.93 cm^{-1} are attributed to the pyranose cycle of cellulose. The CTA-NW is confirmed with the appearance of peaks for C=O, $CH(CH_3)$, C–O of acetyl groups of wave numbers 1,712, 1,462.9 and 1,240 cm^{-1}, respectively.

3.2. FO setup

The flat sheet FO laboratory setup is shown in Fig. 2. The setup is composed of two channels and a flat membrane taken in sandwich in between. The hydrophilic membrane has an active area of 48×10^{-4} m^2. The thicknesses of the channel on the feed side and on the DS side were 2.5 cm, and the channel length on both sides was 9.5 cm. The FS and DS flow rate were fixed at 20 L h^{-1}. FS and DSs were circulated on either side of the membrane using a variable speed peristaltic pump (Masterflex L/S). A constant temperature water bath was used to keep the feed and DSs at constant temperature during the experiment. The water flux was calculated by measuring the increase in the volume of DS each hour. The rate at which the volume increases divided by the membrane area yields the water flux:

$$J_w = \frac{\Delta V}{A \times \Delta t} \tag{16}$$

where ΔV (L) is the volume change of FS over a fixed time Δt (h) and A is the effective FO membrane area (m^2).

The rejection ratio (rate), R, is then calculated from the following equation:

$$R = 100 \times \left(1 - \frac{C_p}{C_F}\right) \tag{17}$$

where R is the solute rejection, C_p (mg L^{-1}) is the permeate concentration, C_F (mg L^{-1}) is the solute concentration in the FS determined by atomic absorption spectrometry for measuring the concentration of Cr(VI).

3.3. Feed and draw solutions

The FS consisted of potassium dichromate ($K_2Cr_2O_7$) dissolved in distilled water and its concentration ranged from 20 to 5,000 mg L^{-1}. The DS consisted of ammonium bicarbonate (NH_4HCO_3), and its concentration ranged from 0.5 to 3 mol L^{-1}. Throughout this study, all prepared solutions were set up in a 200 mL Erlenmeyer flask. The ammonium bicarbonate DS is flowing on the permeate side (support layer) and the $K_2Cr_2O_7$ solution on the feed (active layer) side.

4. Results and discussion

FO experiments were carried out using potassium dichromate and ammonium bicarbonate solutions as FS and DS, respectively. The effect of feed concentration, draw concentration, feed temperature and draw temperature was evaluated on the water flux and retention rate.

Water flux is an important indicator to evaluate the FO performance. In this section, the effect of temperature and solution concentration on the water flux was investigated in the FO process. According to the previous research, we note that the process performance was independent with the FS pH value. A study is done by Wu et al. [24] showed that at all tested pH, mercury removal was found to be consistent, approximately 92%. In addition, increasing the pH had no influence on water flux. Moreover, Zhang et al. [25] were found that, in the pH range between 2 and 9, the water permeation flux and the phenolic compounds rejection were independent with the FS pH value.

4.1. Effect of feed concentration

We fixed the draw concentration at 0.5 mol L^{-1} in ambient temperature and we varied the feed concentration. The water flux was examined under four different feed concentrations 6.8×10^{-5}, 3.4×10^{-4}, 3.4×10^{-3} and 17×10^{-3} mol L^{-1}.

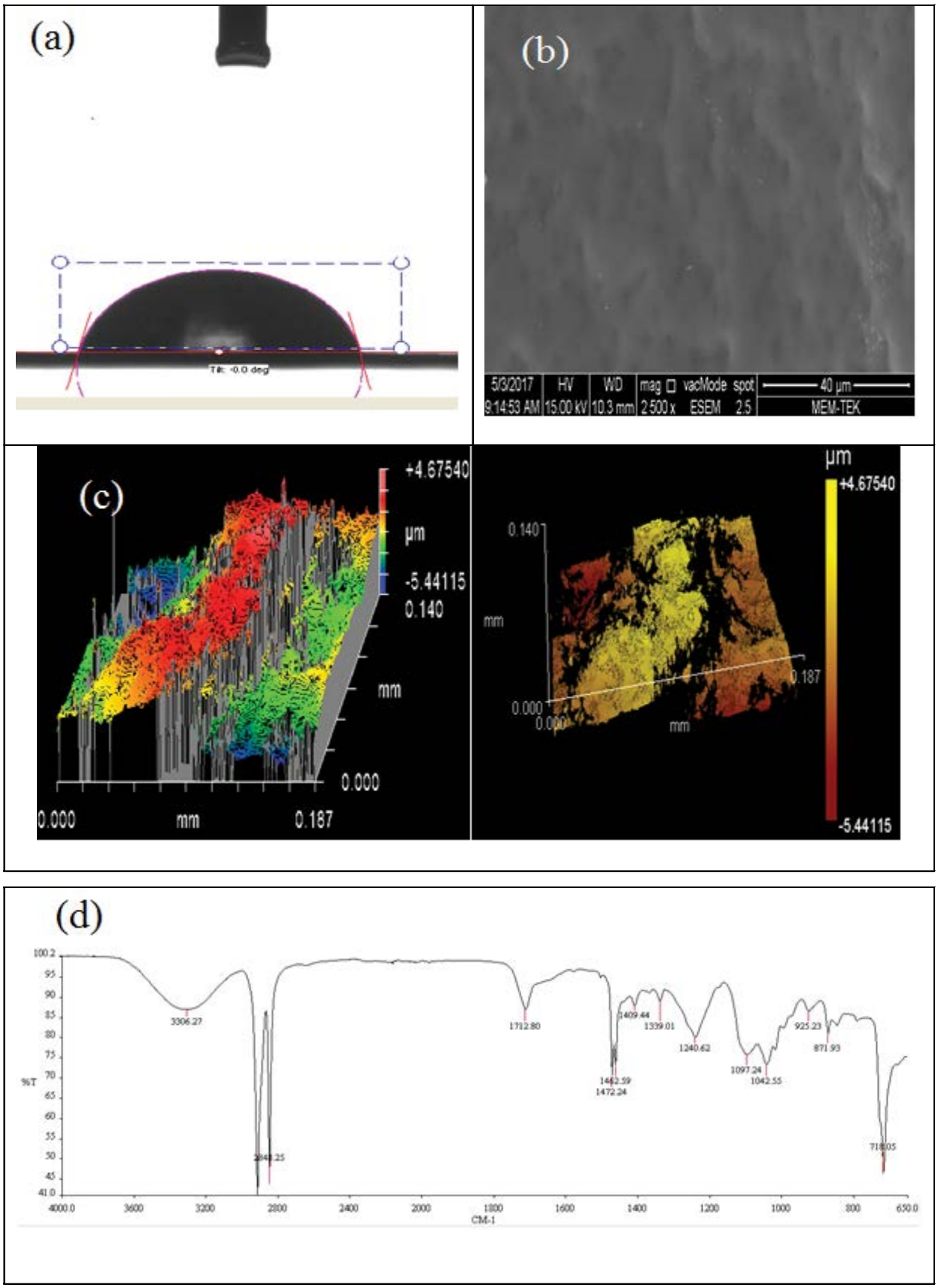

Fig. 1. (a) CA, (b) SEM, (c) profilometer and (d) FTIR spectrum membrane characterization.

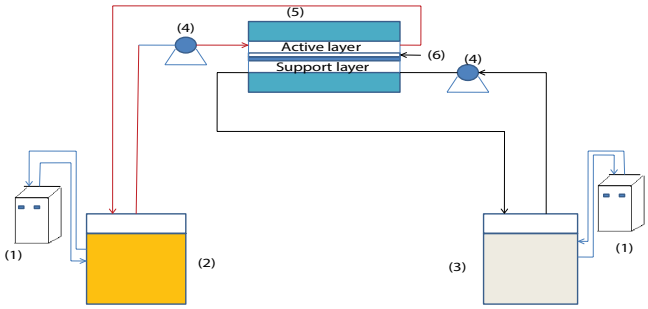

Fig. 2. Schematic diagram of the lab-scale FO system: (1) water bath, (2) feed solution, (3) draw solution, (4) peristaltic pumps, (5) FO membrane cell and (6) FO membrane.

Fig. 3 presents the flux and the retention vs. the feed concentration. It shows a linear decrease of the water flux as function of the feed concentration. The previous experimental observations are in a good agreement with the model (as shown in Fig. 3). The highest J_w value (1.39×10^{-6} m s^{-1}) was calculated for 6.8×10^{-5} mol L^{-1} feed concentration. The water flux is quite high for the tests at low feed concentrations, suggesting that a high feed concentration leads to a decrease in osmotic driving force ($\Delta\pi = \pi_D - \pi_F$), which in turn may significantly reduce the water flux [22,26]. Another study developed by Zhao et al. [27] investigated the influence of FS concentration on the water flux and the removal of organic micro-pollutants. It was found that the water fluxes of phenol and aniline decrease from 4.97×10^{-6} to 4.22×10^{-6} m s^{-1} and from 5.03×10^{-6} to 4.08×10^{-6} m s^{-1}, respectively, when their concentrations increase from 500 to 2,000 ppm. Rejection ratios of phenol and aniline were found to be 73.7% and 91.8%, respectively. Moreover, Cui et al. [28] noted that brackish water with 5, 10, and 20 g L^{-1} NaCl exhibited water fluxes of 2.13, 1.88, and 1.65×10^{-6} m s^{-1}, respectively.

Fig. 3 also presents the rejection of chromium as a function of feed concentration determined from FO experiments. The rejection experiments were conducted to evaluate the influence of the feed concentration on retention rate at similar draw concentration. For an efficient FO process, it is also imperative that chromium rejection be high. All the tests showed a rejection of over 99.92%. The maximum R of 99.98% was achieved when the initial concentration of Cr(VI) was 3.4×10^{-3} and 17×10^{-3} mol L^{-1}. The highest retention of Cr(VI) occurred at 3.4×10^{-3} and 17×10^{-3} mol L^{-1} of initial Cr(VI) and 0.5 mol L^{-1} draw concentration. So, this initial concentration of hexavalent chromium was chosen as the best initial concentration of Cr(VI).

4.2. Effect of DS concentration

Fig. 4 represents the variation of the flux and the retention rate as a function of the concentration of DS for a constant FS concentration (20 mg L^{-1}) and ambient temperature. Fig. 4 shows that the water flux increases with the increase of draw concentration. For a high concentration, we observed an increase in the deviation between the model and the experimental results; whose deviation can be attributed to the enhanced CP effects at higher water flux generated due to higher concentration differences. Recent studies have revealed that operating the FO process above the critical flux could accelerate membrane scaling and membrane fouling [29]. This deviation of the water flux with the DS concentrations has already been reported in many studies [30–33]. The asymptotic trends give the highest value for the permeate flux (2.9×10^{-6} m s^{-1}) for a 3 mol L^{-1} DS concentration. The influence of DS concentration was reported by Nguyen et al. [29], who showed that the water flux increased rapidly from 0.74 to 2.44×10^{-6} m s^{-1} with the increase of the EDTA-2Na concentration from 0.1 to 1 mol L^{-1}.

An increase in draw concentration inducing an increase in driving force should lead to an increase in water flux [34,35] as presented in Fig. 4. Hence, the required concentration of DS is directly related to the FO membrane performance because it is the source of the driving force in the FO process since it has a higher osmotic pressure than the FS [36]. The excellent agreement between the experimental data and the model shows that the model is accurate for the selected FO membrane.

The effect of the DS concentration on the retention of Cr(VI) is presented in Fig. 4, showing that Cr(VI) retention increases slowly with the increase in draw concentration. All the tests show a rejection of over 99.92%. The greatest retention ratio of Cr(VI) occurred at 3 mol L^{-1} of NH_4HCO_3. On the other hand, Benavides and Phillip [37] have used an FO to recover water from an FS and its ability to minimize

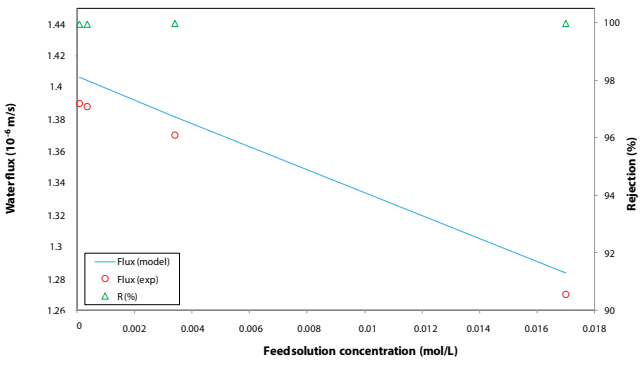

Fig. 3. Water flux and retention rate of chromium vs. concentration of FS.

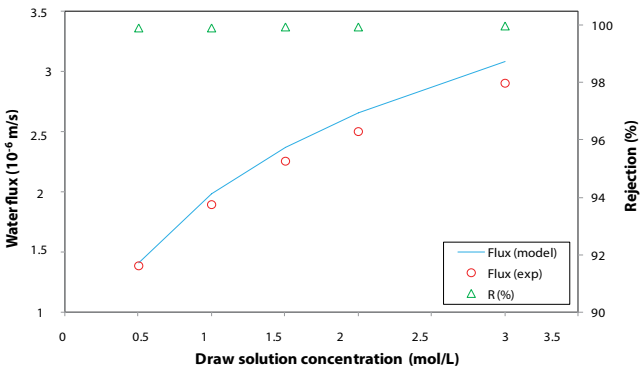

Fig. 4. Concentration of DS vs. water flux and retention rate.

solute leakage. A maximum solute rejection for desalination applications was obtained to be 99.3% [38].

Temperature has a direct effect on the osmotic pressure of the solution and other thermodynamic properties such as diffusion coefficient, viscosity, etc. Since FO process involves two independent feed streams on each side of the membrane, the influence of temperature on each solution may affect the FO process differently. The influence of temperature on the properties of the DS and FS is discussed separately in the upcoming sections [32].

4.3. Effect of DS temperature

Temperature difference was created between the DS and FS by increasing the temperature of the DS, while keeping the temperature of FS at baseline (25°C). The water flux when the FO is operated at different draw temperatures is plotted in Fig. 5, revealing that the temperature has an influence on the water flux.

The flux increases with the temperature of the DS for a constant FS temperature 25°C. The DS temperature varied from 25°C to 55°C, the water flux have increased from 1.39 to 2.38 × 10^{-6} m s^{-1}; whose results are in accordance with the theoretical values. Once again, the theoretical results agree well with the experimental ones. These results indicate that temperature plays a positive role in enhancing the water flux and therefore the performance of FO.

Xie et al. [39] have investigated the effect of temperature on FO membrane flux using rain water as FS and cooling water as DS, the average membrane flux was 0.86 × 10^{-6} m s^{-1} when the temperature of the DS was 50°C and decreased notably to about 0.08 × 10^{-6} m s^{-1} at 3°C.

At different temperatures (25°C, 29°C, 39°C, 48°C and 55°C), the residual Cr(VI) concentrations were determined after 1 h to estimate the effect of temperature. The removal of Cr(VI) at different temperatures is also shown in Fig. 5. It is observed that the maximum retention ratio reaches 99.97% at 48°C and 55°C. Therefore, temperature has no significant effect on the retention ratio of chromium by FO process.

The increase in water flux with temperature can be explained by the Wilke–Chang equation, according to which the diffusion coefficient is proportional to the absolute temperature divided by the viscosity of the solvent. The increase in temperature reduces the viscosity of solution and increases the diffusion coefficients, which results in the increase in water flux [33].

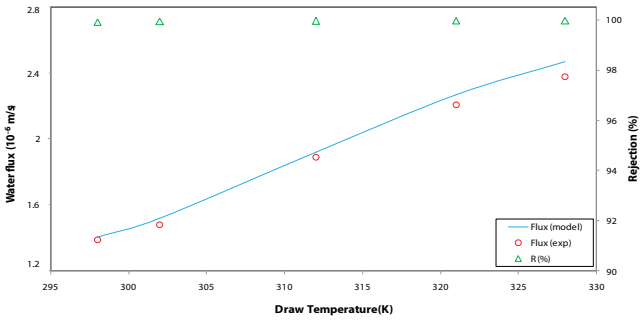

Fig. 5. Water flux and retention rate vs. DS temperature at constant FS temperature of 25°C.

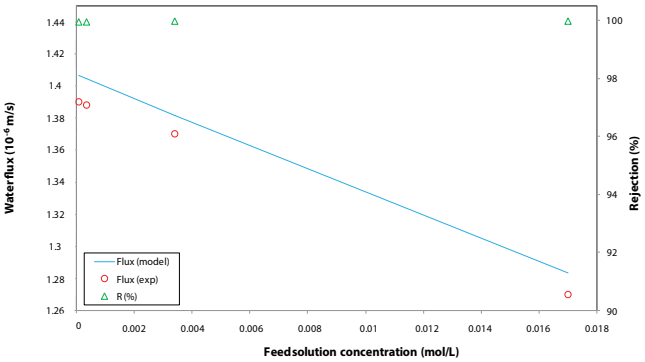

Fig. 6. Water flux and retention rate vs. FS temperature at constant DS temperature of 25°C.

4.4. Effect of FS temperature

FO experiments were conducted under different feed temperatures while keeping the draw temperature constant (25°C). Fig. 6 shows the influence of feed temperature on the water flux of the FO process at various feed temperatures. Water flux increases when the temperature of FS solution was increased from 25°C to 46°C. The increase of water flux is evident at all the tested FS temperatures. In many studies, enhanced water flux at higher temperature was mainly thought to be caused by a decreased water viscosity, which enhances the self-diffusivity of water, and therefore mass transfer coefficient of the FS [9]. Furthermore, a good agreement was noticed between the theoretical and experimental results.

The increase of osmotic pressure of the FS at higher temperature also contributes to a net osmotic pressure decrease across the membrane. The maximum level of the flux was 1.95 × 10^{-6} m s^{-1} at 43°C and the minimum level was 1.39 × 10^{-6} m s^{-1} at 25°C.

Another study was conducted by Wang et al. [40], which assumed that the temperature difference between FS and DS and transmembrane had effect on the rejection of 12 trace organic contaminants (TrOCs) by two FO membranes. It has been found that the feed temperature has an important effect on the increase of the permeate flux. For instance, increasing the feed temperature from 20°C to 40°C caused an increase in water flux from 1.53 × 10^{-6} to 2.22 × 10^{-6} m s^{-1}.

Fig. 6 shows that the increase of feed temperature has no significant effect on the retention rate of chromium. In this case, the retention rate varied slightly with the temperature. So, it has so important technical implications that FO membranes can achieve higher solute retention ratio independently of the operating temperature.

5. Conclusion

In this study, the effects of temperature and concentration on FO performance water flux and retention ratio were evaluated, using NH_4HCO_3 as DS and $K_2Cr_2O_7$ as FS. The obtained results have shown that water flux increases with DS concentration at low FS concentration in the FO mode. In addition, the retention ratio of chromium was found to reach the up-limit of 99.9%. It has been clearly seen

that the temperature and concentration of FS and DS have a negligible effect on the removed chromium. It has been experimentally proven that the effect of the DS temperature is more significant than the FS temperature. The water permeability has showed a higher dependency on the DS temperature.

The performed tests under the standard conditions for FO application have indicated that the increase in both temperature and concentration of DS was the most suitable conditions to improve the FO performance. The validation of the theoretical model represents a good agreement between the predicted and experimental results. The FO process has shown high performance for chromium rejection.

In this study, it has been proven that the chromium can be successfully removed from wastewater by FO process. In addition, ammonium bicarbonate can be considered as efficient DS for the chromium removal by FO. Despite the good performance in terms of retention ratio, the increase in the flux and longevity of the membrane remains the major challenge for the FO application.

Acknowledgment

The authors would like to thank Mrs Leila MAHFOUDHI, major teacher of English in the Sfax Faculty of Sciences, for proofreading and polishing the language of the manuscript.

Symbols

A	—	Membrane pure water permeability coefficient, m Pa^{-1} s^{-1}
C	—	Molar concentration of the solution, mol L^{-1}
C_F	—	Solute concentration in the feed solution, mol L^{-1}
C_P	—	Permeate concentration, mol L^{-1}
D_D	—	Diffusion coefficient of draw solute, m^2 s^{-1}
D_F	—	Diffusion coefficient of the feed solute, m^2 s^{-1}
d_h	—	Hydraulic diameter of the flow channel, m
J_w	—	Water flux, m s^{-1}
k	—	Mass transfer coefficient, m s^{-1}
K	—	Solute resistivity for diffusion within the porous support layer, s m^{-1}
k_b	—	Boltzmann constant, 1.380×10^{-23} J K^{-1}
L	—	Channel length of FO test cell, m
n	—	Van't Hoff factor
P_w	—	Hydrated perimeter, m
R	—	Gas constant, $R = 0.0821$ L atm mol^{-1} K^{-1}
r	—	Ion radius, m
R	—	Solute rejection, %
Re	—	Reynolds number
S	—	Area of the flow section, m^2
S	—	Structural parameter of the membrane, m
Sc	—	Schmidt number
Sh	—	Sherwood number
T	—	Absolute temperature of the solution, K
t	—	Thickness of the support layer, m
T_D	—	Temperature of the draw solution, K
T_F	—	Temperature of the feed solution, K
CP	—	Concentration polarization
FS	—	Feed solution
DS	—	Draw solution
FO	—	Forward osmosis
CTA	—	Cellulose triacetate
TFC	—	Thin-film composite membrane

Greek

ρ	—	Density of the solution, kg m^{-3}
μ	—	Dynamic viscosity, kg m^{-1} s^{-1}
ε	—	Porosity of the support layer
σ	—	Reflection coefficient
τ	—	Tortuosity of the support layer
$\Delta\pi$	—	Osmotic driving force, Pa
π_D	—	Osmotic pressure of the draw solution, Pa
π_F	—	Osmotic pressure of the feed solution, Pa
ρ_w	—	Water density, kg m^{-3}
π	—	Osmotic pressure, Pa
v	—	Average flow velocity, m s^{-1}
ϑ	—	Kinematic viscosity of the solution, m^2 s^{-1}

References

[1] Y. Qu, X. Zhang, J. Xu, W. Zhang, Y. Guo, Removal of hexavalent chromium from wastewater using magnetotactic bacteria, Sep. Sci. Technol., 136 (2014) 10–17.
[2] A. Demir, M. Arisoy, Biological and chemical removal of Cr(VI) from waste water: cost and benefit analysis, J. Hazard. Mater., 147 (2007) 275–280.
[3] M. Karnib, A. Kabbani, H. Holail, Z. Olama, Heavy metals removal using activated carbon, silica and silica activated carbon composite, Energy Procedia, 50 (2014) 113–120.
[4] N. Kongsricharoern, C. Polprasert, Chromium removal by a bipolar electro-chemical precipitation process, Water Sci. Technol., 34 (1996) 109–116.
[5] S. Rengaraj, K.-H. Yeon, S.-H. Moon, Removal of chromium from water and wastewater by ion exchange resins, J. Hazard. Mater., 87 (2001) 273–287.
[6] S. Kalidhasan, N. Rajesh, Simple and selective extraction process for chromium (VI) in industrial wastewater, J. Hazard. Mater., 170 (2009) 1079–1085.
[7] F. Fu, Q. Wang, Removal of heavy metal ions from wastewaters: a review, J. Environ. Manage., 92 (2011) 407–418.
[8] A. Bingol, A. Aslan, A. Cakici, Biosorption of chromate anions from aqueous solution by a cationic surfactant-modified lichen (*Cladonia rangiformis* (L.)), J. Hazard. Mater., 161 (2009) 747–752.
[9] M. Bhattacharya, S.K. Dutta, J. Sikder, M.K. Mandal, Computational and experimental study of chromium (VI) removal in direct contact membrane distillation, J. Membr. Sci., 450 (2014) 447–456.
[10] A. Hafiane, D. Lemordant, M. Dhahbi, Removal of hexavalent chromium by nanofiltration, Desalination, 130 (2000) 305–312.
[11] H.-g. Choi, M. Son, H. Choi, Integrating seawater desalination and wastewater reclamation forward osmosis process using thin-film composite mixed matrix membrane with functionalized carbon nanotube blended polyethersulfone support layer, Chemosphere, 185 (2017) 1181–1188.
[12] Y. Cui, Q. Ge, X.-Y. Liu, T.-S. Chung, Novel forward osmosis process to effectively remove heavy metal ions, J. Membr. Sci., 467 (2014) 188–194.
[13] B. Vital, J. Bartacek, J.C. Ortega-Bravo, D. Jeison, Treatment of acid mine drainage by forward osmosis: heavy metal rejection and reverse flux of draw solution constituents, Chem. Eng. J., 332 (2018) 85–91.
[14] P. Zhao, B. Gao, Q. Yue, S. Liu, H.K. Shon, The performance of forward osmosis in treating high-salinity wastewater containing heavy metal Ni^{2+}, Chem. Eng. J., 288 (2016a) 569–576.
[15] X. Liu, J. Wu, C. Liu, J. Wang, Removal of cobalt ions from aqueous solution by forward osmosis, Sep. Purif. Technol., 177 (2017) 8–20.
[16] K.L. Lee, R.W. Baker, H.K. Lonsdale, Membranes for power generation by pressure-retarded osmosis, J. Membr. Sci., 8 (1981) 141–171.

[17] S. Loeb, L. Titelman, E. Korngold, J. Freiman, Effect of porous support fabric on osmosis through a Loeb–Sourirajan type asymmetric membrane, J. Membr. Sci., 129 (1997) 243–249.
[18] T.Y. Cath, A.E. Childress, M. Elimelech, Forward osmosis: principles, applications, and recent developments, J. Membr. Sci., 281 (2006) 70–87.
[19] J.R. McCutcheon, M. Elimelech, Modeling water flux in forward osmosis: implications for improved membrane design, AIChE J. 53 (2007) 1736–1743.
[20] T. Ruprakobkit, L. Ruprakobkit, C. Ratanatamskul, Carboxylic acid concentration by forward osmosis processes: dynamic modeling, experimental validation and simulation, Chem. Eng. J., 306 (2016) 538–549.
[21] K. Touati, F. Tadeo, C. Hanel, T. Schiestel, Effect of the operating temperature on hydrodynamics and membrane parameters in pressure retarded osmosis, Desal. Wat. Treat., 57 (2016) 10477–10489.
[22] J.S. Collura, D.E. Harrison, C.J. Richards, T.K. Kole, M.R. Fisch, The effects of concentration, pressure, and temperature on the diffusion coefficient and correlation length of SDS Micelles, J. Phys. Chem. B, 105 (2001) 4846–4852.
[23] A. Boubakri, S.A.T. Bouguecha, I. Dhaouadi, A. Hafiane, Effect of operating parameters on boron removal from seawater using membrane distillation process, Desalination, 373 (2015) 86–93.
[24] C.-Y. Wu, H. Mouri, S.-S. Chen, D.-Z. Zhang, M. Koga, J. Kobayashi, Removal of trace-amount mercury from wastewater by forward osmosis, J. Water Process Eng., 14 (2016) 108–116.
[25] X. Zhang, Q. Lia, J. Wang, J. Li, C. Zhao, D. Hou, The main aim of this part is to determine the optimal operating conditions, in which the water flux and the retention rate were relatively high, J. Environ. Chem. Eng., 5 (2017) 2508–2514.
[26] S. Phuntsho, F. Lotfi, S. Hong, D.L. Shaffer, M. Elimelech, H. Kyong Shon, Membrane scaling and flux decline during fertiliser-drawn forward osmosis desalination of brackish groundwater, Water Res., 57 (2014) 172–182.
[27] P. Zhao, B. Gao, Q. Yue, S. Liu, H.K. Shon, Effect of high salinity on the performance of forward osmosis: water flux, membrane scaling and removal efficiency, Desalination, 378 (2016) 67–73.
[28] Y. Cui, X.Y. Liu, T.S. Chung, M. Weber, C. Staudt, C. Maletzko, Removal of organic micro-pollutants (phenol, aniline and nitrobenzene) via forward osmosis (FO) process: evaluation of FO as an alternative method to reverse osmosis (RO), Water Res., 91 (2016) 104–114.
[29] H.T. Nguyen, N.C. Nguyen, S.S. Chen, H. Ngo, W. Guo, C.W. Li, A new class of draw solutions for minimizing reverse salt flux to improve forward osmosis desalination, Sci. Total Environ., 538 (2015) 129–136.
[30] S. Phuntsho, H.K. Shon, S.K. Hong, S.Y. Lee, S. Vigneswaran, A novel low energy fertilizer driven forward osmosis desalination for direct fertigation: evaluating the performance of fertilizer draw solutions, J. Membr. Sci., 375 (2011) 172–181.
[31] T.S. Chung, S. Zhang, K.Y. Wang, J. Su, M.M. Ling, Forward osmosis processes: yesterday, today and tomorrow, Desalination, 287 (2012) 78–81.
[32] J.R. McCutcheon, R.L. McGinnis, M. Elimelech, Desalination by ammonia–carbon dioxide forward osmosis: influence of draw and feed solution concentrations on process performance, J. Membr. Sci., 278 (2006) 114–123.
[33] S. Phuntsho, H.K. Shon, S. Vigneswaran, J. Kandasamy, S.K. Hong, S.Y. Lee, Influence of temperature and temperature difference in the performance of forward osmosis desalination process, J. Membr. Sci., 415–416 (2012) 734–744.
[34] G.T. Gray, J.R. McCutcheon, M. Elimelech, Internal concentration polarization in forward osmosis: role of membrane orientation, Desalination, 197 (2006) 1–8.
[35] K.Y. Wang, M.M. Teoh, A. Nugroho, T.S. Chung, Integrated forward osmosis–membrane distillation (FO–MD) hybrid system for the concentration of protein solutions, Chem. Eng. Sci., 66 (2011) 2421–2430.
[36] S. Choua, R. Wanga, L. Shi, Q. Shea, C. Tanga, A.G. Fane, Thin-film composite hollow fiber membranes for pressure retarded osmosis (PRO) process with high power density, J. Membr. Sci., 389 (2012) 25–33.
[37] S. Benavides, W.A. Phillip, Water recovery and solute rejection in forward osmosis modules: modeling and bench-scale experiments, J. Membr. Sci., 505 (2016) 26–35.
[38] J.R. McCutcheon, R.L. McGinnis, M. Elimelech, A novel ammonia—carbon dioxide forward (direct) osmosis desalination process, Desalination, 174 (2005) 1–11.
[39] M. Xie, W.E. Price, L.D. Nghiem, M. Elimelech, Effects of feed and draw solution temperature and transmembrane temperature difference on the rejection of trace organic contaminants by forward osmosis, J. Membr. Sci., 438 (2013) 57–64.
[40] W. Wang, Y. Zhang, M. Esparra-Alvarado, X. Wang, H. Yang, Y. Xie, Effects of pH and temperature on forward osmosis membrane flux using rainwater as the makeup for cooling water dilution, Desalination, 351 (2014) 70–76.

Appendix: Sample of calculation

We have: d_h = 0.003 m; S = 0.000968 m; velocity = 0.0010101 m s^{-1}; L = 0.095 m; r_D = 1.52 × 10^{-10} m; r_F = 1.02667 × 10^{-10} m

- Temperature difference was created between the DS and FS by elevating the temperature of draw solution while keeping the temperature of feed solution at baseline (25°C). For T_D = 302 K:

  A = 1.38 × 10^{-12} m Pa^{-1} s^{-1}; ρ_w = 995.935098 kg m^{-3}; ρ = 996.256895 kg m^{-3}; μ = 0.000817273 kg m^{-1} s^{-1}; v = 8.20343 × 10^{-7} m^2 s^{-1}; Re = 116.9749465; D_D = 1.78155 × 10^{-9}; D_F = 2.60269 × 10^{-9}; Sc = 0.316374939; Sh = 2.162042906; k = 1.87571 × 10^{-6}; K = 543346.238; J_w = 1.5179 × 10^{-6} m s^{-1}

- Temperature difference was created between DS and FS by elevating the temperature of feed solution while keeping the temperature of draw solution at baseline (25°C). For T_F = 302 K:

  A = 1.38 × 10^{-12} m Pa^{-1} s^{-1}; ρ_w = 995.935098 kg m^{-3}; ρ = 996.256895 kg m^{-3}; μ = 0.000817273 kg m^{-1} s^{-1}; v = 8.20343 × 10^{-7} m^2 s^{-1}; Re = 116.9749465; D_D = 1.75796 × 10^{-9}; D_F = 2.63762 × 10^{-9}; Sc = 0.312184543; Sh = 2.133406576; k = 1.87571 × 10^{-6}; K = 550,639.4761; J_w = 1.4978 × 10^{-6} m s^{-1}

- We fixed the draw concentration at 0.5 mol L^{-1} in ambient temperature and we varied the feed concentration. For [feed] = 0.000340136 mol L^{-1}:

  A = 1.325 × 10^{-12} m Pa^{-1} s^{-1}; ρ_w = 997.042 kg m^{-3}; ρ = 998.682116 kg m^{-3}; μ = 0.000893494 kg m^{-1} s^{-1}; v = 8.94673 × 10^{-7} m^2 s^{-1}; Re = 107.2565905; D_D = 1.60799 × 10^{-9}; D_F = 2.38066 × 10^{-9}; Sc = 0.376304846; Sh = 2.357942316; k = 1.87115 × 10^{-6}; K = 601993.9742; J_w = 1.4047 × 10^{-6} m s^{-1}

- We fixed the feed concentration at 6.80272 × 10^{-5} mol L^{-1} in ambient temperature and we varied the draw concentration. For [draw] = 1 mol L^{-1}:

  A = 1.325 × 10^{-12} m Pa^{-1} s^{-1}; ρ_w = 997.042 kg m^{-3}; ρ = 1306.52383 kg m^{-3}; μ = 0.000893494 kg m^{-1} s^{-1}; v = 6.83871 × 10^{-7} m^2 s^{-1}; Re = 140.3182148; D_D = 1.60779 × 10^{-9}; D_F = 2.38066 × 10^{-9}; Sc = 0.219866815; Sh = 1.802366526; k = 1.43027 × 10^{-6}; K = 601993.9742; J_w = 1.9854 × 10^{-6} m s^{-1}